(4)

GL-TR-90-0106

Frequency Dependence and Spatial Distribution of Seismic Attenuation in France: Experimental Results and Possible Interpretations

M. Campillo
J. L. Plantet

Radiomana - Societe Civile
27 Rue Claude Bernard
75005 Paris, FRANCE

12 September 1989

Scientific Report No. 2

GEOPHYSICS LABORATORY
AIR FORCE SYSTEMS COMMAND
UNITED STATES AIR FORCE
HANSCOM AIR FORCE BASE, MASSACHUSETTS 01731-5000

SPONSORED BY
Defense Advanced Research Projects Agency
Nuclear Monitoring Research Office
ARPA ORDER NO 5299

MONITORED BY
Geophysics Laboratory
AFOSR-87-0331

This technical report has been reviewed and is approved for publication.

JAMES F. LEWKOWICZ
Contract Manager
Solid Earth Geophysics Branch
Earth Sciences Division

JAMES F. LEWKOWICZ
Branch Chief
Solid Earth Geophysics Branch
Earth Sciences Division

FOR THE COMMANDER

DONALD H. ECKHARDT, Director
Earth Sciences Division

Unclassified
SECURITY CLASSIFICATION OF THIS PAGE

REPORT DOCUMENTATION PAGE

Form Approved OMB No. 0704-0188

1a. REPORT SECURITY CLASSIFICATION Unclassified	1b. RESTRICTIVE MARKINGS
2a. SECURITY CLASSIFICATION AUTHORITY	3. DISTRIBUTION/AVAILABILITY OF REPORT Approved for public release Distribution unlimited
2b. DECLASSIFICATION/DOWNGRADING SCHEDULE	
4. PERFORMING ORGANIZATION REPORT NUMBER(S)	5. MONITORING ORGANIZATION REPORT NUMBER(S) GL-TR-90-0106
6a. NAME OF PERFORMING ORGANIZATION Radiomana - Société Civile 6b. OFFICE SYMBOL (If applicable)	7a. NAME OF MONITORING ORGANIZATION European Office of Aerospace and Development
6c. ADDRESS (City, State, and ZIP Code) 27 rue Claude Bernard 75005 Paris France	7b. ADDRESS (City, State, and ZIP Code) Box 14 FPO New York 09510 - 0200
8a. NAME OF FUNDING/SPONSORING ORGANIZATION Geophysics Laboratory 8b OFFICE SYMBOL (If applicable)	9. PROCUREMENT INSTRUMENT IDENTIFICATION NUMBER AFOSR - 87 - 0331 - A
8c. ADDRESS (City, State, and ZIP Code) Hanscom AFB MA 01731 - 5000	10. SOURCE OF FUNDING NUMBERS PROGRAM ELEMENT NO. 61101 E PROJECT NO. 7 A 10 TASK NO D A WORK UNIT ACCESSION NO C Z

11. TITLE (Include Security Classification)
Frequency dependence and spatial distribution of seismic attenuation in France : experimental results and possible interpretations.

12. PERSONAL AUTHOR(S)
M. Campillo and J.L. Plantet

13a. TYPE OF REPORT	13b. TIME COVERED	14. DATE OF REPORT (Year, Month, Day)	15. PAGE COUNT
Scientific Report #2	FROM 7/15/88 TO 7/14/89	1989 September 12	56

16. SUPPLEMENTARY NOTATION

17. COSATI CODES		
FIELD	GROUP	SUB-GROUP

18. SUBJECT TERMS (Continue on reverse if necessary and identify by block number)
Seismic waves - Regional phases - Lg, Pg phases - Attenuation - Q factor - Scattering - Crust -

19. ABSTRACT (Continue on reverse if necessary and identify by block number)

We processed digital records from 431 earthquakes at 25 stations of LDG network in France. We computed spectral amplitudes of Pg and Lg in different group velocity windows. We used this large data set to compute a map of mean crustal attenuation by evaluating simultaneously source amplitude, site response and apparent Q.
We used a procedure combining an iterative reconstruction technique with an adjustment of source amplitudes and site responses at each step of the inversion. The stability of the results is tested with different subsets of data and the resolution is evaluated. We obtained maps of apparent attenuation at frequencies between 1.5 and 10 Hz, computed from Pg, Lg and early coda of Lg.
The results obtained are in a good agreement with the predictions of the single scattering model both for frequency dependence and Qs-Qp ratio. The comparison between the attenuation anomaly found in the Variscan belt and a deep reflexion seismic profile confirms the prominant part played by scattering for the apparent attenuation of seismic waves in the crust.

20. DISTRIBUTION/AVAILABILITY OF ABSTRACT ☒ UNCLASSIFIED/UNLIMITED ☐ SAME AS RPT ☐ DTIC USERS	21. ABSTRACT SECURITY CLASSIFICATION Unclassified
22a. NAME OF RESPONSIBLE INDIVIDUAL James Lewkowicz	22b. TELEPHONE (Include Area Code) (617) 377 - 3028 22c. OFFICE SYMBOL GL - LWH

DD Form 1473, JUN 86 *Previous editions are obsolete.* SECURITY CLASSIFICATION OF THIS PAGE
Unclassified

Keywords; Seismic data/reflection; Earth crust; Regional phases; Seismic attenuation/scattering. (EDC)

A

CONTENTS

ILLUSTRATIONS

Illustrations

Frequency dependence and spatial distribution of seismic attenuation in France: experimental results and possible interpretations.

M. Campillo
Laboratoire de Geophysique Interne et Tectonophysique Universite Joseph Fourier and Observatoire de Grenoble IRIGM, BP 53X, 38041 Grenoble, France
J.L. Plantet
Laboratoire de Detection Geophysique Commissariat a l'Energie Atomique BP 12, 91680 Bruyere-le-Chatel, France

Abstract:

We processed digital records from 431 earthquakes at 25 stations of LDG network in France. We computed spectral amplitudes of Pg and Lg in different group velocity windows. We used this large data set to compute a map of mean crustal attenuation by evaluating simultaneously source amplitude, site response and apparent Q. We used a procedure combining an iterative reconstruction technique with an adjustment of source amplitudes ans site responses at each step of the inversion. The stability of the result is tested with different subsets of data and the resolution is evaluated. We obtained maps of apparent attenuation at frequencies between 1.5 and 10 Hz, computed from Pg, Lg and early coda of Lg.

The results obtained are in a good agreement with the predictions of the single scattering model both for frequency dependence and Qs-Qp ratio. The comparison between the attenuation anomaly found in the Variscan belt and a deep reflexion seismic profile confirms the prominant part played by scattering for the apparent attenuation of seismic waves in the crust.

Introduction

The short period seismic phases Pg and Lg have been extensively studied for the purposes of nuclear test monitoring, magnitude determination or attenuation measurements (e.g. Nuttli,1973,1986). Considering regions in which a flat layering can be regarded as a reasonable model for the earth crust, the mode of propagation of these phases has been clearly established by the comparison between observed and theoretical properties. The theoretical results were obtained considering oversimplified models of the crust which consist of stacks of a few flat visco-elastic layers, each of them being considered as homogeneous at any scale. Nevertheless, these numerical simulations fail to explain several very general features of regional phases. The long duration of the signals (the existence of a coda) in most of the observations is not accounted for. Similarly, to explain the actual attenuation of these signals, it is necessary to include in the models a frequency dependent quality factor that is not compatible with accepted processes of intrinsic attenuation at depth. These phenomena are generally attributed to the scattering due to unprecisely defined heterogeneities that have to be added to the vertical layering usually hypothesized. The description of crustal heterogeneity can be separated into two parts. The first one deals with the small scale heterogeneity that consists of the fluctuations of the elastic properties at a scale roughly equal or smaller than the wavelengths considered in short period seismology. These fluctuations cannot be described in a deterministic point of view because the detail of the crustal structure is far beyond our present knowledge. The implications of this type of heterogeneity were studied in detail, particularly to explain the coda of local seismograms and the frequency dependence of the apparent attenuation. Since the pionneering work of Aki (1969), it has been now clearly established that scattering on small fluctuations of elastic parameters can account, at least partially, for the existence of coda and for the frequency dependence of apparent attenuation (see Herraiz and Espinoza (1986) for a review). Most of the developments of the theory of coda waves concern the perturbations of an homogeneous medium. This represents a severe limitation to the interpretation since the earth presents a strong vertical heterogeneity. The importance of the layering for scattered waves was investigated by Wang and Herrmann (1988) and theoretical developments in this domain remain of crucial importance for the understanding of propagation at regional distances. The most obvious effect of the stratification on the scattered field is the generation of surface waves.

Large scale shallow irregularities such as sedimentary basins also produce the local conversion of body waves into propagating surface waves (Campillo, 1987). Nevertheless, because of the large observed attenuation near the surface (Toksoz et al., 1988) and the great variability of the thickness of the surface low velocity layer, we expect the short period surface waves to be unable to propagate along paths of several hundreds of kilometers as Pg or Lg do. Various authors have tried to numerically infer the effect of deep irregularities, such as Moho uplifts, on short period Lg (Kennett, 1984; Campillo, 1987; Maupin, 1989). Their basic conclusion is that Lg appears to be a robust and stable phase even when strong lateral variations of the crustal structure occur. In view of this result, the Lg wavetrain could be used to measure the mean attenuation in the crust. Solely, a measure of the apparent attenuation does not bring much information about the cause and the mechanism of seismic attenuation. An approach to move farther on can be to correlate the characteristics of the attenuation in different regions with the different particular crustal structures encountered. In order to avoid spurious differences that can be produced when comparing measurements made with different types of data or with different techniques, we choose to use an inversion process and a large homogeneous data set. To this end, we have to collect enough data to be able to describe the attenuation in both space and frequency domains, beneath an area sufficiently large to include different geological units.

We have obtained from the LDG seismic network a data set sufficient to cover a great part of France. We require unclipped seismograms showing an acceptable signal to noise ratio in the epicentral distance range 200-1000 km. Because of the dynamic range of the network and the modest seismicity of France this represents long observation time. In a previous study (Campillo, 1987), we used a limited number of earthquakes (18) and of stations (22) to study a region of central France. Because of the small number of records available at that time, we applied the backprojection technique to construct a map of apparent attenuation. We shall discuss these results in a following section. In this study, we have widely increased the data set and the area studied. We will use an iterative SIRT-type reconstruction technique to determine source amplitude and quality factors. We also consider early coda of Lg and Pg waves. Gupta et al. (1989) studied the distribution of Q from Lg in eastern North America assuming a regionalization based on Bouguer gravity contours and geological maps.

Data Processing

We selected 431 earthquakes in France and in its vicinity (Figure 1). These events were recorded at 26 short period vertical seismometers of the LDG network. Unfortunately we have never recorded simultaneously in good conditions at more than 20 stations. The records were collected during the period 1985-1987. For each record, we computed the density of spectral amplitude for four phases defined by the group velocity windows:

6.2 km/s> V > 5.6 km/s	Pg
3.6 km/s> V > 3.1 km/s	Lg1
3.1 km/s> V > 2.6 km/s	Lg2

2.6 km/s> V > 2.3 km/s   Lg3

At this stage, we eliminated the traces where glitchs were detected. For each record, we also computed the density of spectral amplitude of the noise in a window of 30 sec before the first arrival. For a given phase and a given frequency, the spectral density is validated if the signal to noise ratio is greater than 3.

Data Analysis

We model the spectral amplitude observed at station j for earthquake i in the form:

$$A_{i,j}(f,d) = S_j(f) * E(d) * AA_{i,j}(f,d) * St_i(f) \quad (1)$$

where d represents the epicentral distance, f the frequency and:

-$S_j(f)$ = the source excitation. We neglect the radiation pattern due to the focal mechanism as well as the directivity effect associated with rupture propagation. The directivity is known to be a strong effect only on wavelengths much smaller than the source dimension. The Pg and Lg wavetrains are made up of arrivals corresponding to very different take-off angles and therefore the radiation pattern is, in general very smoothed for these phases.

-E(d) = the geometrical spreading of the phase considered in the time domain. After numerical investigations in flat layered models, we found (Campillo et al., 1984):

$$E(d) = d^{-0.83} \text{ for Lg}$$

and (2)

$$E(d) = d^{-1.5} \text{ for Pg}$$

We assume in our analysis that Pg and Lg propagate mostly along straight ray paths i.e. that the mean velocity of S-waves in the crust is roughly constant. Therefore we neglect the effect of focusing-defocusing that was recognized for surface waves (e.g. Zeng et al., 1987).

-$AA_{i,j}(f,d)$ = the apparent attenuation that we express in the form:

$$AA_{i,j}(f,d)=\exp-\left(\frac{\pi f}{V}\int_{d}\frac{d\ell}{Q(f,x,y)}\right) \quad (3)$$

where V is the group velocity and Q the quality factor. This term includes the intrinsic attenuation but also other types of attenuation such as scattering, or propagation effects in a heterogeneous crust that affect the geometrical spreading.

-$ST_i(f)$ = the station response that represents the amplification due to site effects at a given station. The azimuthal dependence of the site response is neglected.

We performed data analysis, then constructed the map of the quality factor independently for each frequency. The first step of our analysis was to assume that the quality factor is constant over the area considered. Then we evaluated the mean quality factor, the source excitation and the station response by an iterative process similar to the scheme used by Campillo et al. (1985). At first, we performed a linear regression to compute Q and S for each earthquake. When the correlation coefficient obtained is smaller than 0.8, the event is eliminated. This value allows us to remove some erroneous data that were kept after our previous sorting, but it can also lead to exclusion of data corresponding to sharp propagation anomalies. We accept this risk because we believe that the anomalous zones are well known and are located outside our study zone. In order to avoid wrong determinations of the source excitation, we use only the data for which the earthquake was recorded by at least 5 stations. An additional condition is that the difference of epicentral distance between the closest and the farthest station is larger than 40 per cent of the largest epicentral distance.

The results obtained at this stage are used as a starting model for an iterative reconstruction that will be described in the next section. The mean values of Qs that we get from Lg are very similar to our previous results (Campillo et al., 1985) and show the same frequency dependence (Qs varies as the square-root of the frequency). Nevertheless, the fact that we are willing to cover a large area with a dense set of paths limits the frequency range available. In fact we can work properly only with frequencies larger than 1 Hz. Figure 2 shows an example of the effective path coverage for a frequency of 3 Hz, after sorting out the data set.

Algorithm of inversion

This algorithm is based on the use of an iterative reconstruction technique that allows us to consider large data sets on small computers. The general scheme of the complete processing is presented in Figure 3. Stage I, as denoted in Figure 3 was discussed in the last section and consists of setting up a starting model with an homogeneous Q(f). In the next stage, we compute a set of Q values at the nodes of a regular grid to describe the actual continuous distribution of apparent attenuation.

After stage I we use equation 1,the expression for the apparent attenuation and the estimations of S and St to evaluate parameter l:

$$l_k = \int_{d_k} \frac{d\ell}{Q(f,x,y)}$$

The set of the l_k-s will be used to invert Q(f,x,y).

The inversion techniques used are slightly modified versions of backprojection and simultaneous iterative reconstruction technique. We shall briefly describe them.

Backprojection and S.I.R.T. operate for a given unknown $Q(f,x,y)=Q_i$ corresponding to location $X_i=(x,y)$ and with the data from the neighbouring paths. Following Mason (1981), we define a circle of influence around Xi. Each path contributes with a weighting coefficient proportional to its length within the circle of influence. This approach is particularly well adapted to the present problem since we know the important part played by scattered waves and multipathing in the propagation of regional phases.

The backprojection is then slightly modified by using the expression:

$$Q_i^{-1} = \frac{\sum_{r=1}^{N_i} a_{r,i} \dfrac{l_r}{L_r}}{\sum_{r=1}^{N_i} a_{r,i}} \qquad (4)$$

where N_i is the number of pathes that cross the circle of influence centered in X_i, $a_{r,i}$ is the length of the path in the circle and L_r is its total length. We compute Q values at the locations X_i for which the number of rays is larger than N_{min}. A supplementary condition is that these rays are coming from a number of distinct sources larger than N_{Smin}. When these conditions are not satisfied, the mean value of Q is assumed. Without further precision, the results presented here are computed with N_{min} equal to 15 and N_{Smin} equal to 8.

Following Cote (1988), we implemented an iterative inversion basically derived from S.I.R.T. (Gilbert, 1972). After the (j-1)th iteration we compute the estimation of l in the jth model: l_r^{j-1}. We define the residue by:

$$res_r^j = l_r - l_r^{j-1}$$

The jth iteration consists of applying to Q^{-1} at location X_i the correction:

$$\delta(Q_i^{-1})^j = \frac{\phi(e_i)}{e_i} \sum_{r=1}^{N_i} a_{r,i} \frac{res_r^j}{L_r}$$

with: (5)

$$e_i = \sum_{r=1}^{N_i} a_{r,i} g_i(\theta_r)$$

and where θ_r is the azimuth of the path r and f and g are weigthing functions which we are about to describe.

$g(\theta_r)$ represents the azimuthal weighting:

$$g_i(\theta_r) = G + (1-G)\ (N_i - D_i(\theta_r))\ /\ N_i$$

where $D_i(\theta_r)$ is the number of paths whose directions are in the range $(\theta_r - 10^\circ, \theta_r + 10^\circ)$ and which intersect the circle of influence centered in X_i. G is a constant that controls the amplitude of the variation of the weighting and that we chose in practice equal to 0.5. The effect of g is to temperate the influence of strong heterogeneities in the distribution of rays.

The damping factor $\phi(e_i)$ varies with the location and depends mainly on the density of rays as:

$$\phi(e_i) = R + (1-R)\ e_i\ /\ e_{max}$$

where e_{max} is the maximum value of the cumulated weighting factors at each point computed over the entire region studied. R is a constant chosen to be equal to 0.5 in the following examples. By using a spatially dependent damping we want to limit the variations of the model in zones where the path coverage is poor. This is specially useful considering the uncertainties implied by our parametrization of the problem as will be discussed in the next section. We have also performed tests where we added a constant to the weighting term e_i, as proposed by Comer and Clayton (1987) who suggested that this operation may stabilize the solution. In our case, this damping affects the convergence rate but has a very weak influence on the final image.

After a series of iterations to actualize the current Q model, we compute the mean residues associated with each station and each earthquake. Next, the station responses and the source excitations are corrected by terms equal to these biases multiplied by damping factors. The values of these damping factors, relative to the mean damping applied for the inversion of Q alone, can be evaluated by comparing the partial derivatives of the amplitude with respect to Q_i, S and St in equation 1. In practice the coefficients of damping ε_S and ε_{St}, as well as the number of iterations on Q_i only, are chosen after numerous trials. We have studied systematically the influence of damping factors and number of internal iterations on the final misfits between model prediction and actual observations. To this aim, we repeated the inversion process tens of times with different parameters. In the following examples we have taken ε_S between 0.06 and 0.04, ε_{St} between 0.03 and 0.02, and the number of iterations of SIRT on Q_i only, equal to 3. With these values the complete scheme converges in about 20 iterations.

Accuracy of the results

As pointed out before, the parameters of the inversion were chosen by trial and error for the specific data set considered. After these numerical tests, it appears that applying strong damping on source excitation and station response corrections warrant the stability and the convergence of the process. The Q model obtained when the process has converged to a mimimum root mean square residue is weakly sensitive to the parameters of damping used, at least when the number of data is large enough. We will illustrate the importance of reaching a critical number of data by considering independant subsets of records of phase Lg1 at a frequency of 3 Hz. We performed the inversion with 4 different sets of data. The number of sources whose records are used in the inversion are: 25, 25, 55 and 100. In the case of the 25 earthquakes subsets, we reduced N_{min} to 8 and N_{Smin} to 3 in order to cover an area comparable to that of the other cases. The Q models obtained are presented in Figure 4. The result computed from the global data set is shown in Figure 6 (Lg1). The results obtained with the two subsets of 25 events are clearly in contradiction. On the opposite, the main features of the Q-distribution computed with the entire set of records are defined correctly when using only 55 or 100 earthquakes. We interpret this very strong dependence of the stability of the solution on the number of data by two characteristics of the technique of measurement used here. The first point concerns the representation of the term of geometrical spreading by a simple smooth functional dependence (equation 2). This is an oversimplification even for synthetic Lg seismograms whose amplitudes exhibit large spatial fluctuations due to interferences, as shown in Campillo et al. (1984). The functional form of the spreading was defined by least squares over a large range of epicentral distance. The second point is that we make an assumption of azimuthal independence of both source excitation and site response that results in a poor precision of isolated attenuation measurements. These points explain why the measurements,and therefore the inversion reaches statistical significance only for large data sets. In our first attempt to infer the attenuation in a limited part of France through a simple backprojection (Campillo, 1987), the number of events considered was too small. Nevertheless, even if some of the maps of Q were erroneous, the general conclusions of the study are confirmed by our new results, as will be shown later.

In order to add a control on the solution obtained for the entire data set, we constructed maps of resolution computed as follows. Considering a model of Qs, S and St, we changed arbitrarily the value of Qs_i , computed the new residues and operated 3 iterations of the global inversion process (that includes perturbations on source excitation and station response values). We plotted the perturbations obtained on Qs to verify if the trade-off between the parameters results in specific unrealistic deformation of the image. We obtained a map for each location X_i. A perfectly decoupling process must produce a perturbation completly concentrated in X_i. The results obtained are presented in Figure 5 for 6 different locations. These maps give a critical view of our results; the perturbations are far to be perfectly concentrated. Nevertheless, the perturbation occurs mostly in the region around the point considered with very small effects in remote regions. This means that we can draw a relatively optimistic conclusion: our maps are very smoothed and therefore represents a long wavelength image of the distribution of the quality factor, but on the other hand the inversion process does not produce strong spurious anomalies.

The last point that we need to discuss for an objective presentation of our results is the misfits between observed and predicted values. Our main interest in this study is the mapping of Qs. We have seen that to infer Qs we also need to compute source excitation and station response. Considering these two last terms as a part of our model, we can compute directly from the actual spectral amplitude an apparent Qs^{-1} value for each record that we compare with the value predicted by the heterogeneous Q model. All misfits due to source or stations are included in this comparison. The fact that we compute the misfits directly in term of Qs^{-1} allows to compare the amplitude of the unresolved fluctuations of the data with the amplitude of the spatial variations of Qs^{-1} obtained from our inversion. For a frequency of 3 Hz, we found in a model with homogeneous Qs^{-1} a standard deviation of $8\ 10^{-4}$ for a mean Qs^{-1} of $1.8\ 10^{-3}$. After the inversion, the standart deviation is reduced to $4.5\ 10^{-4}$.

This indicates the significancy of the quality factor fluctuations with respect to the average misfit of the data.

Results obtained at 3 Hz

We have performed the inversion for the 4 time windows defined previously at the same frequency of 3 Hz. The results obtained are presented in Figure 6. The lowest Q values are reached for Qp deduced from Pg waves. This result is somewhat surprising. As it is generally admitted that the values of intrinsic Q are larger for P waves than for S waves, another cause of apparent attenuation is required to understand this result. One possible explanation is that the Pg phase is more sensitive than the Lg phase to lateral large scale heterogeneity in the crust. This can be explained by the fact that P-waves incident on the Moho can always be refracted in the upper mantle while S-waves are trapped in the crust in a wide range of incident angle. Nevertheless, as we will see later, considering the frequency dependance will lead us to invoke the scattering in a randomly inhomogeneous medium to interpret our results. The distribution of Q inferred from Pg does not exhibit strong variations at 3 Hz. The results obtained with the records corresponding to the window Lg1 are more contrasted. The zones of high attenuation correspond to the perialpine region, the central Massif and more surprisingly an area in the North western corner of the region studied that we will identify later as the Central Armorican Zone. This example illustrates the difficulty to base a regionalization of Q on surface geology only. We shall examine later the frequency dependence for Pg and Lg.

We also present in Figure 6 the results obtained for the windows Lg2 and Lg3 that correspond to the early coda of Lg. We processed and inverted these data exactly in the same way as we did for Lg1, without taking into consideration their nature of coda waves. For Lg2 the image presents a clear similarity with the results obtained with Lg1. There is a slight increase of the mean value of Qs between Lg1 and Lg2. For Lg3 the image is poorly resolved, although one can distinguish features which are common to Lg1 and Lg2. The interpretation of the results obtained with late arrivals is difficult. Nevertheless, the very close average value of Qs that we found from primary waves (Lg1) and from early coda (Lg2), assuming the same geometrical spreading for both phases suggests that these waves are associated with a only mode of propagation, as discussed in Campillo (1990).

Frequency dependence of Qs inferred from Lg1

Figure 7 presents the Qs distributions computed at different frequencies. The images are less constrasted at high frequency in addition to the fact that, for high frequencies the contrast between quality factors with large values are much less significant in term of energy attenuation. There are two different features for the patterns shown on the figure. First some patterns have amplitudes that vary strongly with frequency and disappear almost completly at high frequency. This can be explained by the fact that the attenuation is dominated by the effect of scattering, which is known to result in a peak of attenuation in the frequency domain. The anomalous attenuation in the Central Armorican Zone is in this first category. Otherwise, the Alpine and peri-Alpine region seems associated with attenuation whatever the frequency is, although the contrast is more significant for the lowest frequencies. This point suggests the addition of a strong intrinsic attenuation to the scattering effect in this region. Indeed there is a sedimentary basin as deep as 10 km at the western periphery of the Alpine arc. However one cannot neglect the fact that a mountain range like the Alps is associated with large scale crustal heterogeneity. This can affect the geometrical spreading of Lg and result in apparent attenuation.

One conclusion that we can draw from these images is the clear frequency dependance of the mean quality factor and the decrease in amplitude of the spatial variations of Q at high frequency. It was one of the main conclusions of a previous work (Campillo, 1987) to show that apparent attenuation in the crust occurs in a limited frequency band. This result supports the hypothesis that attenuation of crustal waves is caused mainly by scattering on small scale inhomogeneity rather than by factors producing frequency independent effects such as inelasticity or large scale lateral heterogeneity. The distribution of Q follows the trend towards associating tectonically active regions with low Q. But an intriguing problem is , for frequencies between 2 and 8 Hz, the existence of a region of high attenuation beneath the Hercynian basement of western France.

Frequency dependence of Qp inferred from Pg

The results obtained for Qp at 4 different frequencies are presented in Figure 8. The image obtained at 2 Hz is shown only to illustrate the strong frequency dependence of Qp in this frequency range. Actually Qp varies with frequency even faster than Qs. There is a relatively good agreement between the patterns obtained for Qp and Qs, although the images obtained for Qp are less contrasted. This seems to indicate that, in spite of the different absolute values obtained for Qs and Qp, the causes of attenuation are the same for the two types of waves.

Discussion of the mean values of apparent Qs

Qp inferred from Pg is smaller than Qs obtained from Lg1 over the whole frequency range. We can interpret both apparent attenuations in terms of intrinsic attenuation and scattering effect. If we consider the mean values of the quality factors we find that the frequency dependance is stronger for Qp than for Qs. As this is also true for the different regions we will discuss only the results obtained for the mean values. This does not mean that the inversion is useless, on the contrary it allows a better evaluation of source excitations and station responses and therefore a more accurate measurement of Q.

The frequency dependence cannot be directly analyzed because anelasticity and scattering are both acting with *a priori* unknown strength. In fact we can make reasonable assumptions about the frequency dependence of these two terms. Intrinsic Q has a high value with a very weak frequency dependence as found from measurements in shield areas (Nuttli, 1982; Singh and Herrmann, 1983; Hasegawa, 1985). Sato (1984), under a single scattering assumption, predicted that scattering Q varies with the frequency for wavelenghths smaller than the correlation distance. In the same paper Sato showed that his theoretical results are in agreement with the observations made in different active regions. Assuming that we deal with wavelength smaller than the correlation distance, Sato's results indicate that the scattering Q is expected to be larger for S waves than for P waves and it is effectively our observation. We have substracted from our results the effect of the intrinsic attenuation that we consider to be represented by a constant Q of 1500. After this correction we find Qs^{scatt} and Qp^{scatt} to be proportional to the frequency in the range 2 Hz-10 Hz as shown in Figure 9. The ratio between quality factors of S and P waves (about 1.5) is not as large as predicted by Sato (1984): 2.41. If we assume a correlation distance of 2 km, our results indicate a mean fluctuation of 5% when measured from S waves and of 4% when measured from P waves.

These values are actually very close. One can remember that this simple interpretation is done under the assumption that the entire path of the wave is within the randomly inhomogeneous medium. These values can be underestimated if it appears that only a part of the crust is concerned by the scattering. We can conclude from the mean values of the quality factor that there is a good agreement between our experimental results and the theoretical predictions drawn by Sato within the mean wave formalism framework.

Discussion of the spatial distribution of apparent attenuation

We have discussed our results in terms of average values for the entire area and the whole depth of the crust. We may now try to understand the distribution of the apparent quality factor. One of the main features of our image is the attenuative character of the Alpine region. Nevertheless we have seen that the poor resolution of our inversion in this area that does not allow a detailed analysis of this very complex region. It is a well known observation that active mountain ranges are associated with low Q. A more puzzling feature is the existence of a region of attenuating material elongated in the direction NW-SE in the north-western part of France. This pattern is neither correlated with the surface geology nor with the distribution of seismicity (Figure 1 gives a realistic view of the seismicity). The direction of elongation corresponds to the structural direction of the Variscan basement in this region (Matte and Hirn, 1988). The deep crustal structures are known in this region since the "ECORS Nord de la France" experiment which consisted of a vertical reflection seismic profile and of a wide angle profile. The records obtained with this last technique have been interpreted by Matte and Hirn (1988). Their profile crosses the low Q region that we found in northwestern France. This is a very fortunate opportunity to compare the apparent attenuation of the crust in a given region with its heterogeneity as revealed by seismic exploration. The part of the seismic section that corresponds to the intersection with the zone of higher attenuation is characterized by a very specific seismic signature as shown in Figure 10. This zone is bounded by two faults that seem to cross the entire crust. The reflections from the lower crust are numerous and have large amplitudes, indicating strong impedance contrasts. This comparison between the image produced by seismic reflection experiment and the apparent attenuation supports the hypothesis that scattering plays an important part in the attenuation of seismic waves within the crust. Indeed this agreement may be fortuitous but it is the only example of such a comparison that we can make with our data set.

An interesting feature of this comparison is that it indicates a correlation between the apparent attenuation of multiply reflected crustal waves and the heterogeneity of the lower crust. The heterogeneity of the lower crust is revealed by its large reflectivity in most of the examples of deep reflexion profiles (e.g. Brown et al., 1986; Peddy and Hobbs, 1987). On the contrary the upper crust is generally more transparent to seismic waves. The strong scattering of short period waves in the crust could be localized in the region of strong reflectivity, i.e. the lower crust. A controversial hypothesis can be drawn: most of the attenuation occurs in two regions of the crust: the first few kilometers beneath the surface as suggested by Toksoz et al. (1988) and the highly inhomogeneous lower crust as shown in our study. The fact that an important part of apparent attenuation of S waves originates in the possibly ductile lower crust is consistent with the explanation of the temporal variation of coda Q proposed by Jin and Aki (1989).

Conclusion

We have shown that a precise measurement of Qs or Qp from regional phase records requires the processing of a large data set. The very large trade-off between the unknowns necessitates a very careful interpretation of the results of the inversion. We believe that the inversion may be also useful to increase the accuracy of the measurement of the mean value of the quality factors. We have shown that the relatively poor resolution of our inversion results in an important smoothing of the image but does not produce artefacts.

The results obtained show the frequency dependance of Qp and Qs. A simple analysis shows that the mean values obtained are in agreement with the single scattering model of Sato (1984) which implies a linear dependence of the quality factor with frequency and larger values of Qp than Qs. We found that the mean fluctuation of velocity needed to explain the data is about 5%. The distribution of quality factors is governed by large scale structures such as the alpine range. We found that ancient structures can be associated with zones of high attenuation. The Central Armorican Zone in the Variscan belt is an example of that. Because we have an image of the crustal structure obtained with wide angle reflexion, we can associate the high apparent attenuation in this zone with scattering in a highly heterogeneous lower crust. Such a comparison between the apparent attenuation and the observed heterogeneity of the crust must be repeated to confirm the correlation obtained in this paper. The quality factor tomography is useful for the quantitative interpretation of short period seismic phases but if such a correlation is confirmed, it can also be a promising tool of investigation of deep crustal structures.

AKNOWLEDGMENTS

This work was supported by the Advanced Research Projects Agency and was monitored by the Air Force Office of Scientific Research under Grant 87.0331.

REFERENCES

Aki, K. 1969 Analysis of the seismic coda of local earthquakes as scattered waves. J. Geophys. Res. 74, 615-631.

Brown, L., M. Barazangi, S. Kaufman and J. Oliver 1986 The first decade of COCORP 1974-1984 in "Reflection Seismology: a global perspective", edited by M. Barazangi and L. Brown, AGU Geodyn. Series 13, 107-120.

Campillo, M. 1987 *Lg* wave propagation in a laterally varying crust and the distribution of quality factor in Central France. J. Geophys. Res. 92, 12604-12614.

Campillo, M. 1990 Propagation and attenuation characteristics of the crustal phase Lg. Pure Appl. Geophys. 132

Campillo, M. ,M. Bouchon and B. Massinon 1984 Theoretical study of the excitation, spectral characteristics and geometrical attenuation of regional seismic phases. Bull. Seism. Soc. Am. 74, 79-90.

Campillo, M., J.L. Plantet and M. Bouchon 1985 Frequency dependent attenuation in the crust beneath Central France from Lg waves: data analysis and numerical modelling. Bull. Seism. Soc. Am. 75, 1395-1411.

Comer, R.P. and R.W. Clayton 1987 Reconstruction of mantle heterogeneity by iterative back-projection of travel times I

Theory and reliability. J.G.R

Cote, P 1988 Tomographies sismiques en genie civil, PhD Thesis, Universite Joseph Fourier, Grenoble, France

Gilbert, P. 1972 Iterative Methods for the three dimensional reconstruction of an object from projections. J. theor. Biol 36, 105-117.

Gupta, I.N., K.L. McLaughlin, R.A. Wagner, R.S. Jih and T.W. McElfresh, 1989 Seismic wave attenuation in eastern North America, EPRI RP 2556-9 final report, EPRI, Palo Alto, Ca.

Hasegawa, H.S. 1985 Attenuation of Lg waves in the Canadian shield. Bull. Seism. Soc. Am. 75, 1569-1582.

Herraiz, M. and A.F. Espinoza 1986 Scattering and attenuation of high frequency seismic waves: development of the theory of coda waves. USGS Open-File Report 86-455.

JIN, A. and K. Aki 1989 Spatial and temporal correlation between coda Q^{-1} and seismicity and its physical mechanism, in press J. Geophys. Res.

Kennett, B.L.N. 1984 Guided wave propagation in laterally varying media, I, Theoretical development, Geophys. J. R. Astr. Soc. 79, 235-255.

Mason, I.M. 1981 Algebraic reconstruction of two-dimensional velocity inhomogeneity in the High Hazles seam of Thoresby colliery. Geophysics 46, 298-308.

Matte, P. and A. Hirn 1988 Seismic signature and tectonic cross section of the Variscan crust, Tectonics 7, 141-155.

Maupin, V 1989 Numerical modelling of Lg propagation accross the North Sea central graben, Geophys. J. in press

Nuttli, O. 1973 Seismic wave attenuation and magnitude relations for eastern North America, J. Geophys. Res. 78, 876-885.

Nuttli, O. 1982 The earthquake problem in the eastern United States, J. Struct. Div. Am. Soc. Civ. Eng. 108, 1302-1312.

Nuttli, O. 1986 Yield estimates of Nevada Test Site explosions obtained from seismic Lg waves, J. Geophys. Res. 91, 2137-2151.

Peddy, C.P. and R.W. Hobbs 1987 Lower crustal reflectivity of the continental margin Southwest of Britain. Annales Geophysicae B5, 331-338

Sato, H. 1984 Attenuation and enveloppe formation of three-component seismograms of small local earthquakes in randomly inhomogeneous lithosphere. J. Geophys. Res. 89, 1221-1241.

Singh, S.K. and R.B. Herrmann 1983 Regionalization of crustal coda Q in the continental United States, J. Geophys. Res. 88, 527-538.

Toksoz, M.N., A. Dainty, E. Reuter and R.S. Wu 1988 A model for attenuation and scattering in the earth's crust. Pure Appl. Geophys. 128, 81-101.

Wang, C.Y. and R.B. Herrmann 1988 Synthesis of coda waves in layered medium. Pure Appl. Geophys. 128, 7-42.

Zeng, Y.H., J. Faulkner, T.L. Teng and K. Aki 1987 Focusing and defocusing of Rayleigh waves from USSR across arctic region to US. EOS Trans. AGU, 68, 1377.

Figure Captions

Figure 1: Locations of earthquakes (squares) and stations (black dots) used in this study.

Figure 2: Path coverage at a frequency of 3 Hz.

Figure 3: Scheme of data processing and inversion.

Figure 4: Results obtained with different subsets of 25, 25, 55 and 100 events.

Figure 5: Resolution maps relative to 6 different locations.

Figure 6: Results obtained at 3 Hz for the 4 group velocity windows considered.

Figure 7: Results obtained for the group velocity window Lg1 at different frequencies.

Figure 8: Results obtained for Qp in the group velocity window corresponding to Pg

Figure 9: Frequency dependence of the quality factor for P and S waves after correction of our result from a frequency independent intrinsic Q of 1500.

Figure 10: Wide angle reflection profile showing a zone of strong heterogeneity in the crust (after Matte and Hirn, 1988) and the apparent Qs inferred from Lg (Lg1).

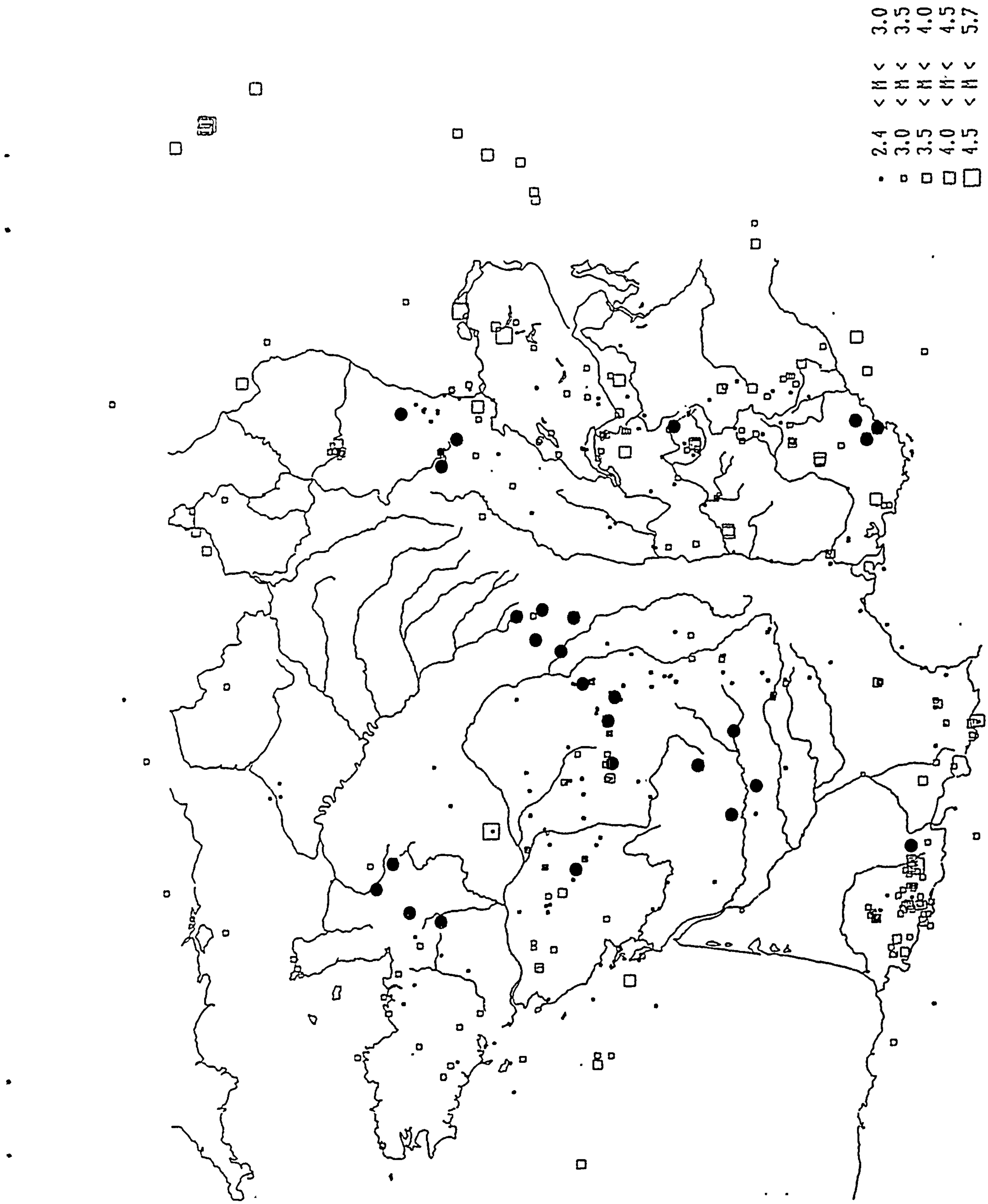

FIGURE 1

FIGURE 2

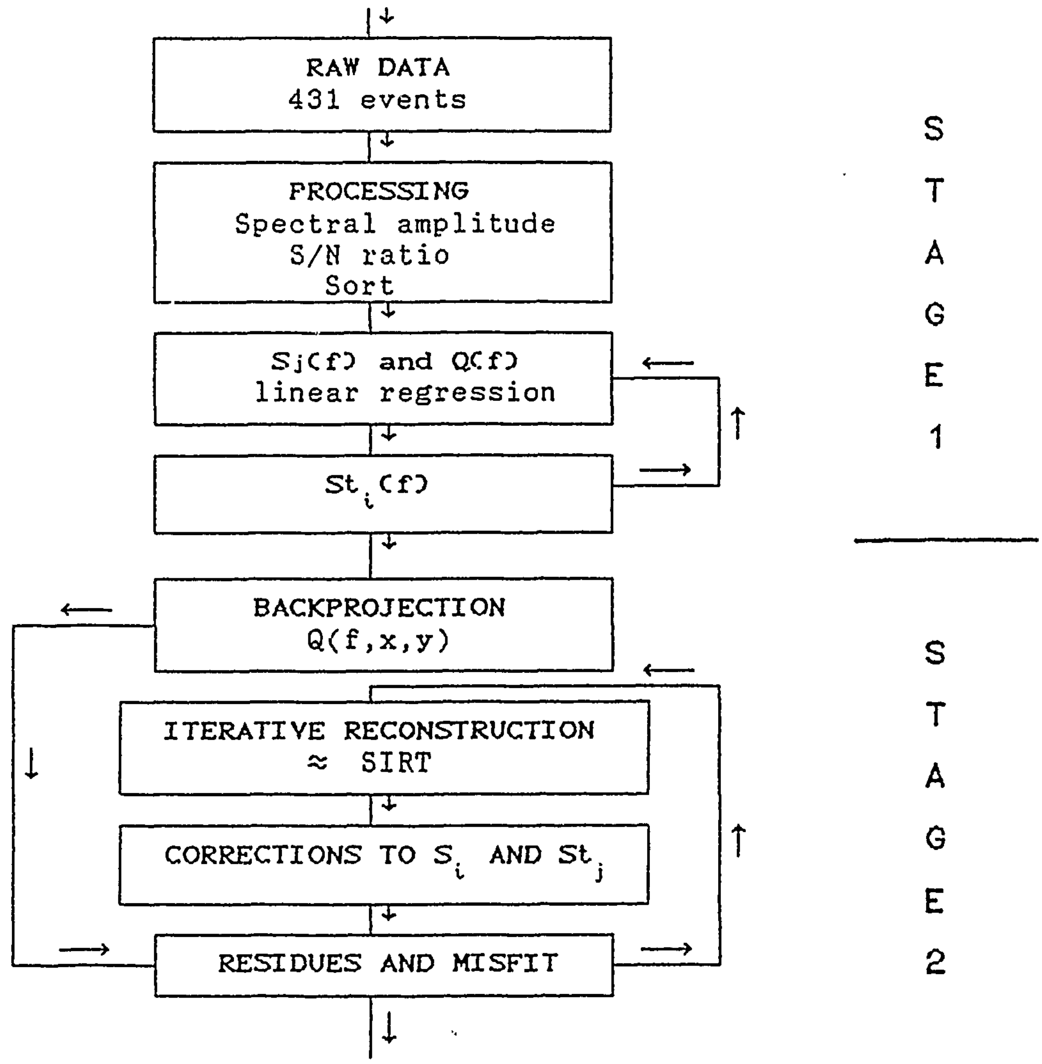

RAW DATA
431 events
PROCESSING
Spectral amplitude
S/N ratio
Sort
Sj(f) and Q(f)
linear regression
$St_i(f)$
BACKPROJECTION
Q(f,x,y)
ITERATIVE RECONSTRUCTION
≈ SIRT
CORRECTIONS TO S_i AND St_j
RESIDUES AND MISFIT
STAGE 1
STAGE 2

FIGURE 3

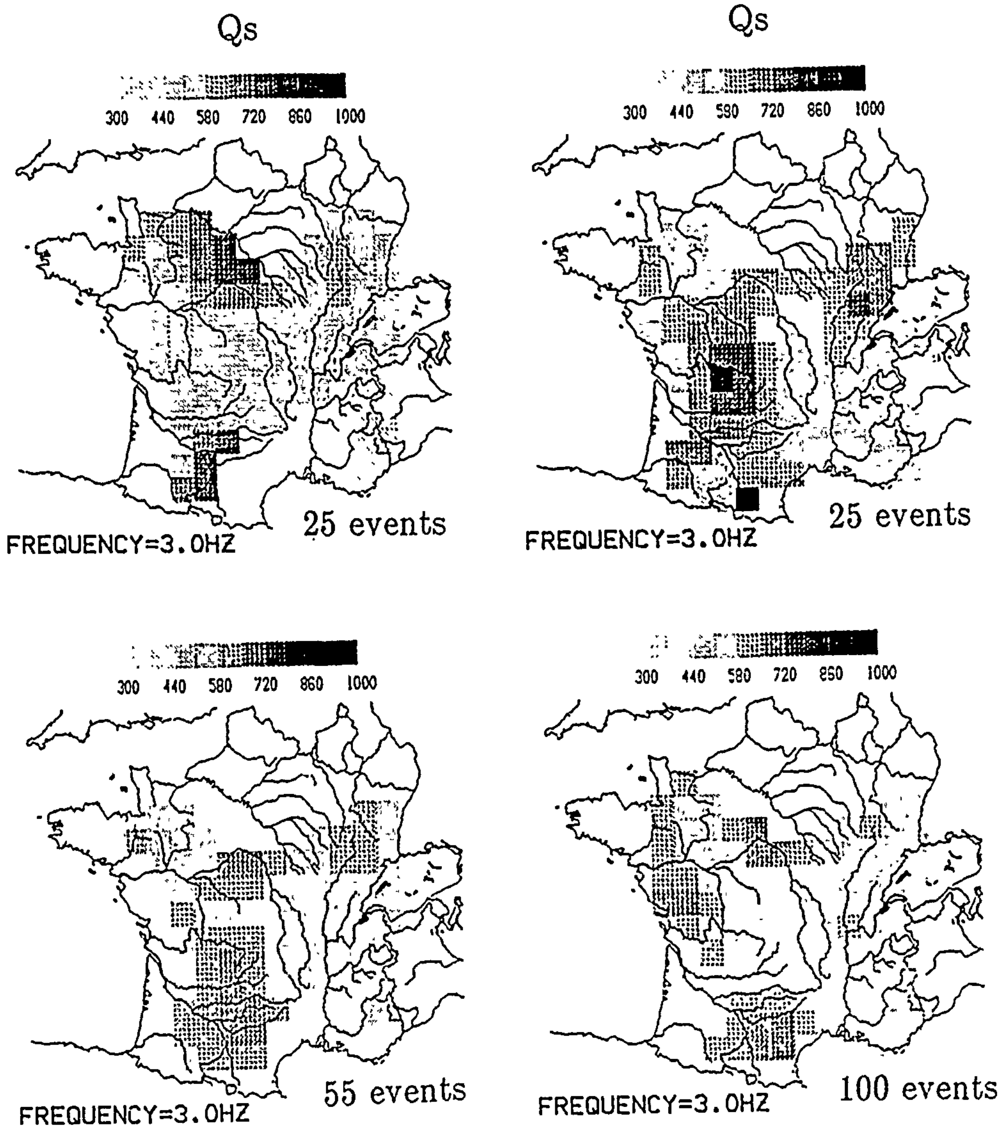
Qs
300 440 580 720 860 1000
FREQUENCY=3.0HZ
25 events
Qs
300 440 580 720 860 1000
FREQUENCY=3.0HZ
25 events
300 440 580 720 860 1000
FREQUENCY=3.0HZ
55 events
300 440 580 720 850 1000
FREQUENCY=3.0HZ
100 events

FIGURE 4

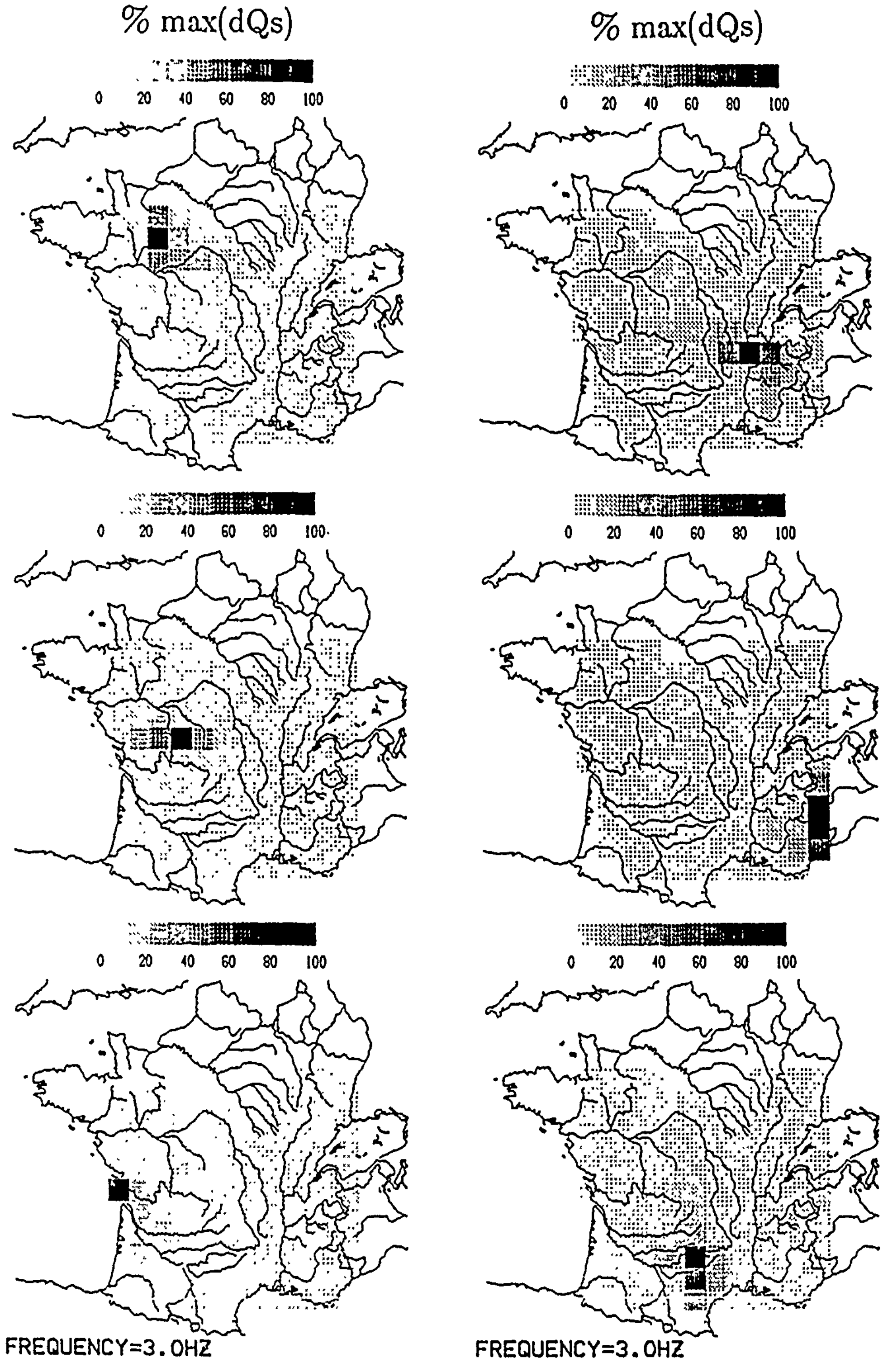
% max(dQs)
% max(dQs)
0 20 40 60 80 100
0 20 40 60 80 100
0 20 40 60 80 100
0 20 40 60 80 100
0 20 40 60 80 100
0 20 40 60 80 100
FREQUENCY=3.0HZ
FREQUENCY=3.0HZ

FIGURE 5

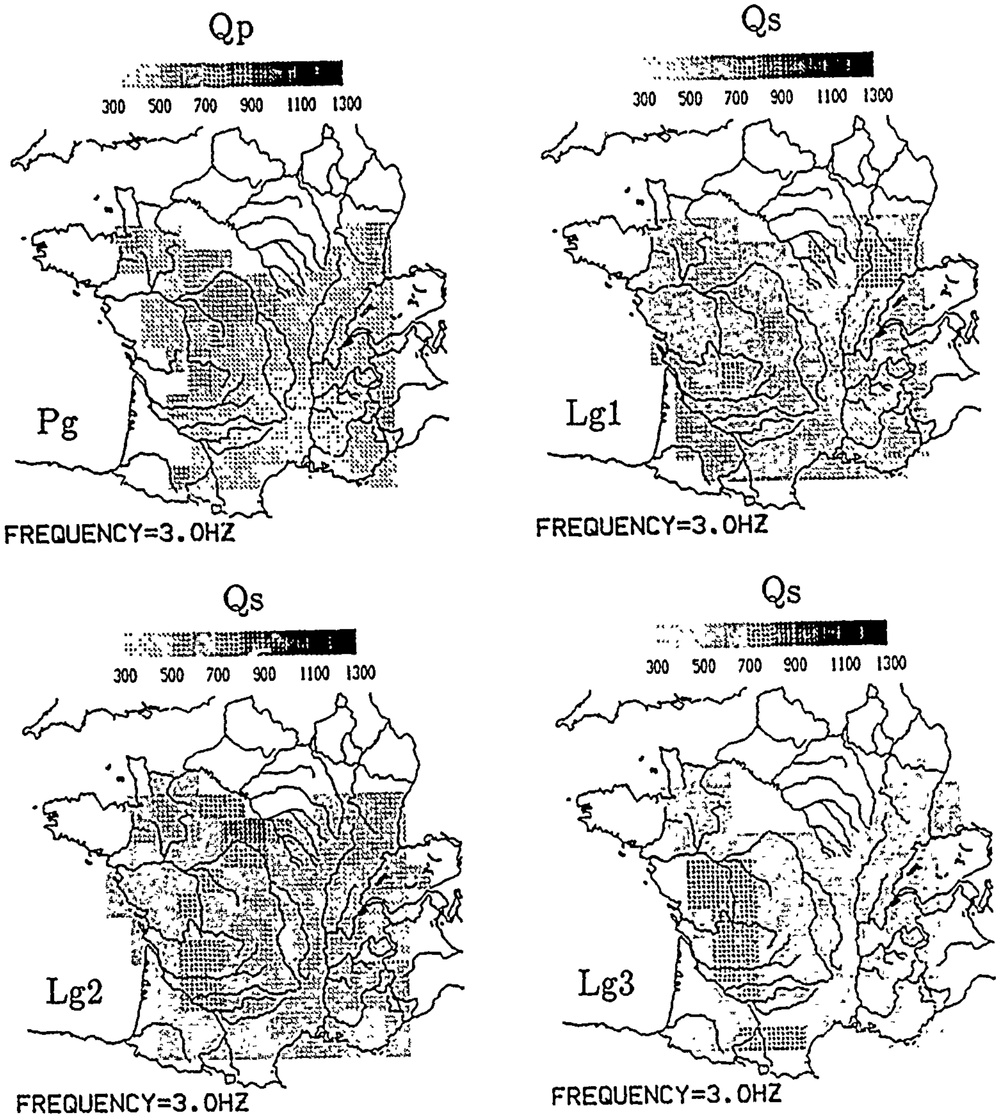
Qp
300 500 700 900 1100 1300
Pg
FREQUENCY=3.0HZ
Qs
300 500 700 900 1100 1300
Lg1
FREQUENCY=3.0HZ
Qs
300 500 700 900 1100 1300
Lg2
FREQUENCY=3.0HZ
Qs
300 500 700 900 1100 1300
Lg3
FREQUENCY=3.0HZ

FIGURE 6

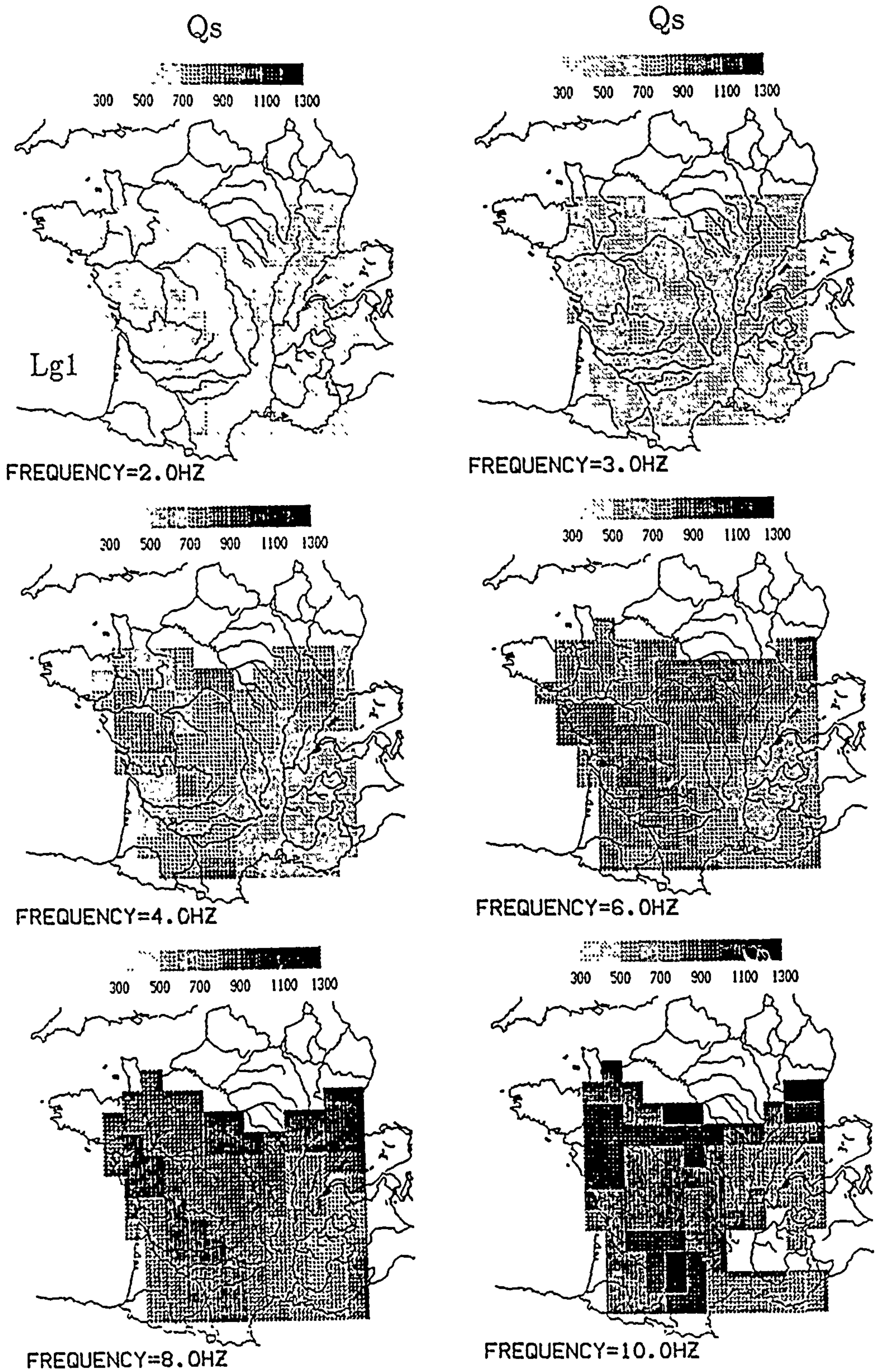
Qs
300 500 700 900 1100 1300
Lg1
FREQUENCY=2.0HZ
Qs
300 500 700 900 1100 1300
FREQUENCY=3.0HZ
300 500 700 900 1100 1300
FREQUENCY=4.0HZ
300 500 700 900 1100 1300
FREQUENCY=6.0HZ
300 500 700 900 1100 1300
FREQUENCY=8.0HZ
300 500 700 900 1100 1300
FREQUENCY=10.0HZ

FIGURE 7

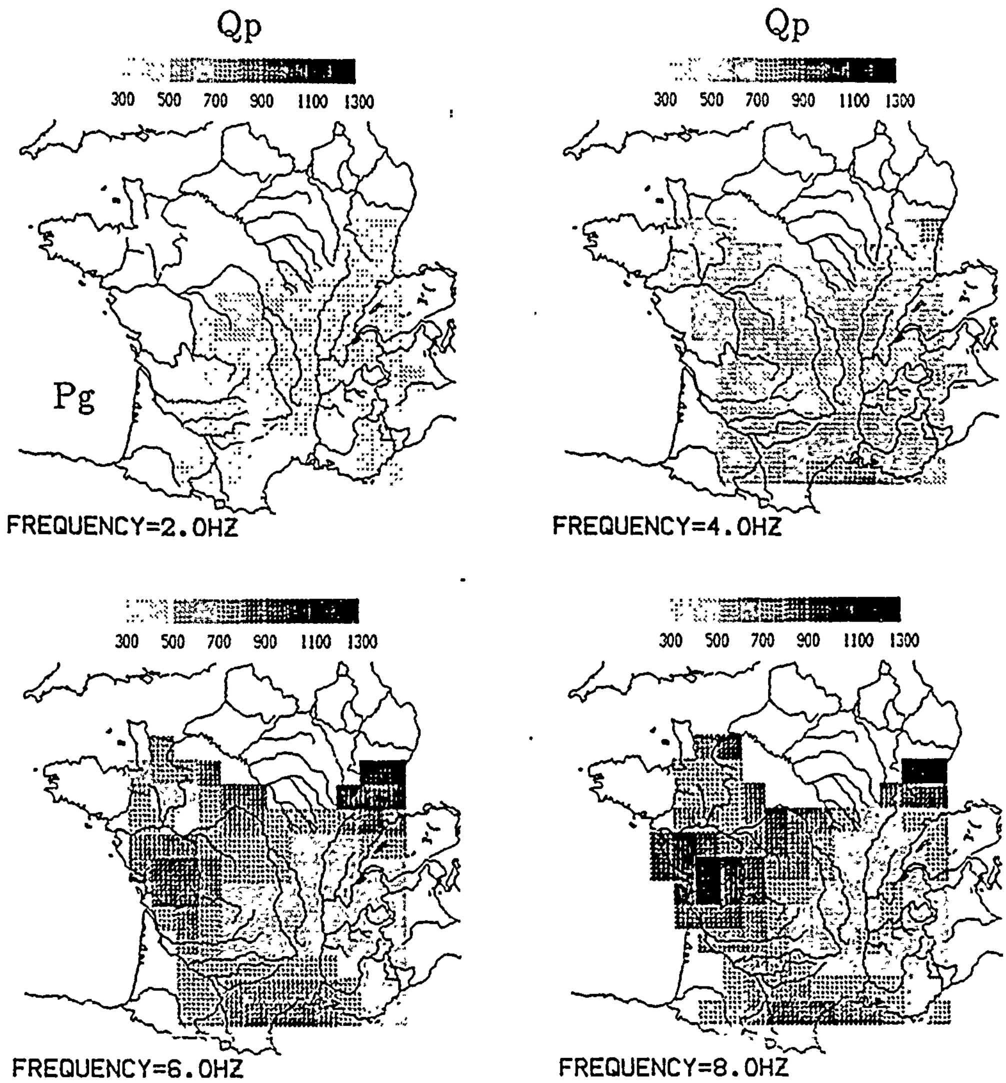
Qp
300 500 700 900 1100 1300
Pg
FREQUENCY=2.0HZ
Qp
300 500 700 900 1100 1300
FREQUENCY=4.0HZ
300 500 700 900 1100 1300
FREQUENCY=6.0HZ
300 500 700 900 1100 1300
FREQUENCY=8.0HZ

FIGURE 8

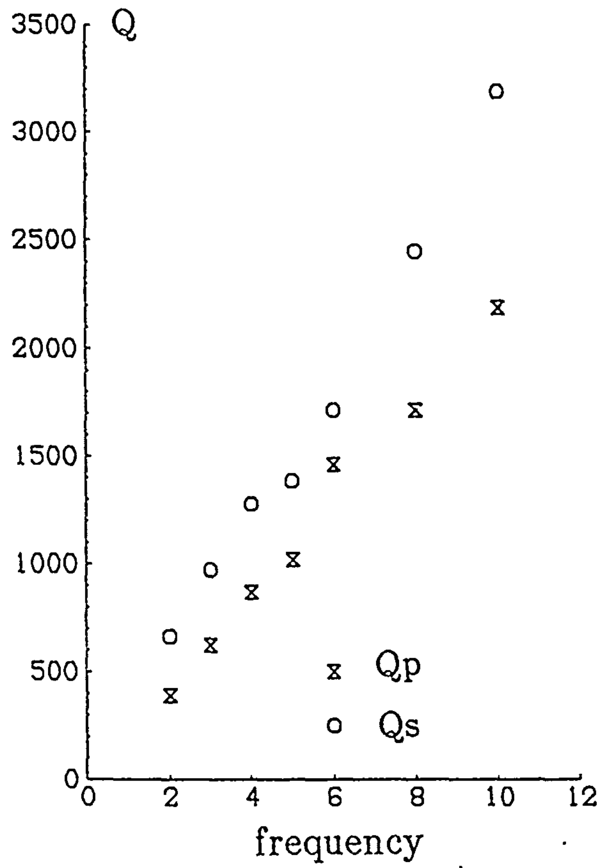

3500
3000
2500
2000
1500
1000
500
0
Q
Qp
Qs
0
2
4
6
8
10
12
frequency

FIGURE 9

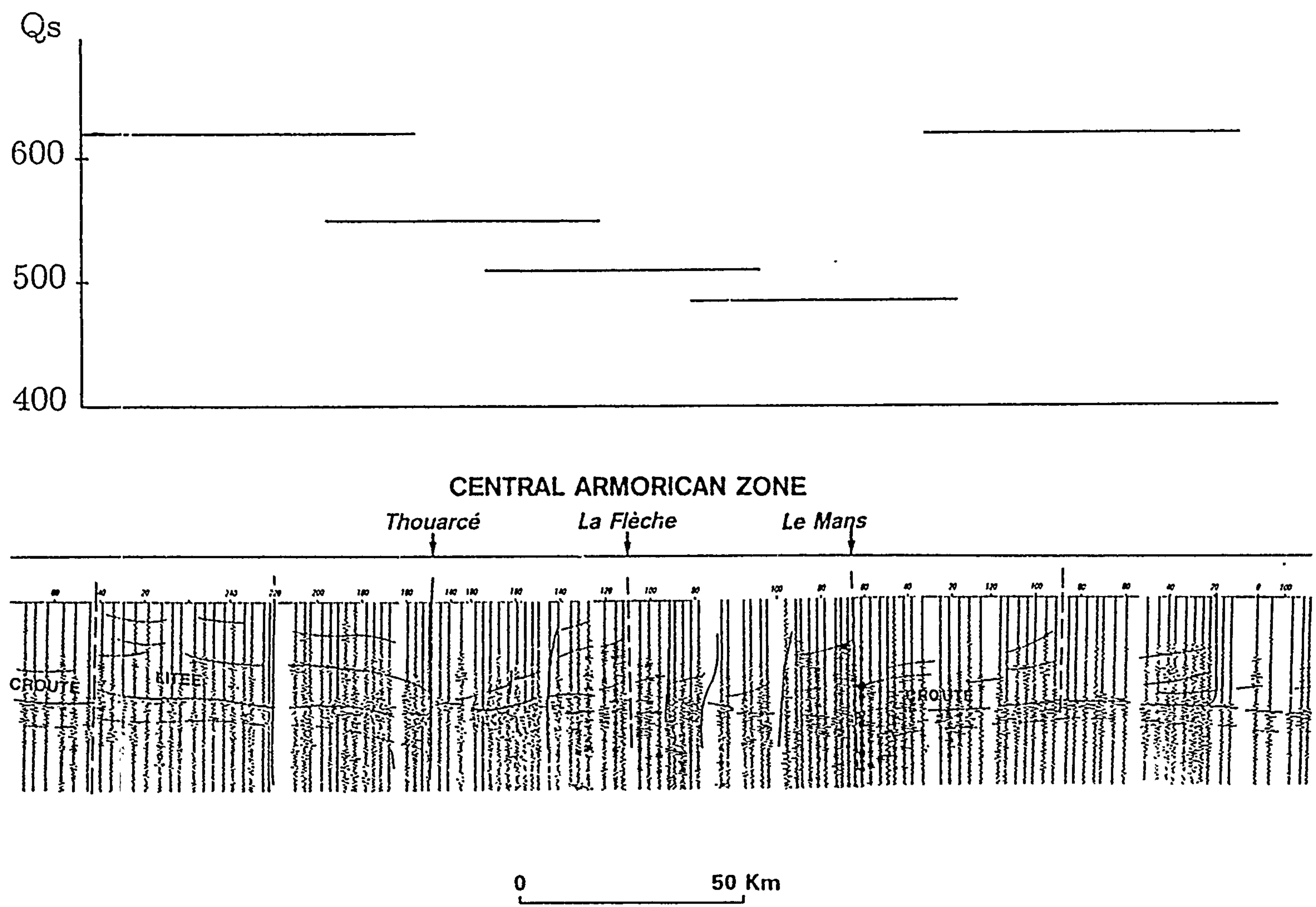

Qs
600
500
400
CENTRAL ARMORICAN ZONE
Thouarcé
La Flèche
Le Mans
CROUTE
CROUTE
0
50 Km

FIGURE 10

Prof. Thomas Ahrens
Seismological Lab, 252-21
Division of Geological & Planetary Sciences
California Institute of Technology
Pasadena, CA 91125

Prof. Charles B. Archambeau
CIRES
University of Colorado
Boulder, CO 80309

Prof. Muawia Barazangi
Institute for the Study of the Continent
Cornell University
Ithaca, NY 14853

Dr. Douglas R. Baumgardt
ENSCO, Inc
5400 Port Royal Road
Springfield, VA 22151-2388

Prof. Jonathan Berger
IGPP, A-025
Scripps Institution of Oceanography
University of California, San Diego
La Jolla, CA 92093

Dr. Lawrence J. Burdick
Woodward-Clyde Consultants
566 El Dorado Street
Pasadena, CA 91109-3245

Dr. Karl Coyner
New England Research, Inc.
76 Olcott Drive
White River Junction, VT 05001

Prof. Vernon F. Cormier
Department of Geology & Geophysics
U-45, Room 207
The University of Connecticut
Storrs, CT 06268

Professor Anton W. Dainty
Earth Resources Laboratory
Massachusetts Institute of Technology
42 Carleton Street
Cambridge, MA 02142

Prof. Steven Day
Department of Geological Sciences
San Diego State University
San Diego, CA 92182

Dr. Zoltan A. Der
ENSCO, Inc.
5400 Port Royal Road
Springfield, VA 22151-2388

Prof. John Ferguson
Center for Lithospheric Studies
The University of Texas at Dallas
P.O. Box 830688
Richardson, TX 75083-0688

Prof. Stanley Flatte
Applied Sciences Building
University of California
Santa Cruz, CA 95064

Dr. Alexander Florence
SRI International
333 Ravenswood Avenue
Menlo Park, CA 94025-3493

Prof. Henry L. Gray
Vice Provost and Dean
Department of Statistical Sciences
Southern Methodist University
Dallas, TX 75275

Dr. Indra Gupta
Teledyne Geotech
314 Montgomery Street
Alexandria, VA 22314

Prof. David G. Harkrider
Seismological Laboratory
Division of Geological & Planetary Sciences
California Institute of Technology
Pasadena, CA 91125

Prof. Donald V. Helmberger
Seismological Laboratory
Division of Geological & Planetary Sciences
California Institute of Technology
Pasadena, CA 91125

Prof. Eugene Herrin
Institute for the Study of Earth and Man
GeophysicalLaboratory
Southern Methodist University
Dallas, TX 75275

Prof . Robert B. Herrmann
Department of Earth & Atmospheric Sciences
St. Louis University
St. Louis, MO 63156

Prof. Bryan Isacks
Cornell University
Department of Geological Sciences
SNEE Hall
Ithaca, NY 14850

Dr. Rong-Song Jih
Teledyne Geotech
314 Montgomery Street
Alexandria, VA 22314

Prof. Lane R. Johnson
Seismographic Station
University of California
Berkeley, CA 94720

Prof. Alan Kafka
Department of Geology & Geophysics
Boston College
Chestnut Hill, MA 02167

Dr. Richard LaCoss
MIT-Lincoln Laboratory
M-200B
P. O. Box 73
Lexington, MA 02173-0073 (3 copies)

Prof Fred K. Lamb
University of Illinois at Urbana-Champaign
Department of Physics
1110 West Green Street
Urbana, IL 61801

Prof. Charles A. Langston
Geosciences Department
403 Deike Building
The Pennsylvania State University
University Park, PA 16802

Prof. Thorne Lay
Institute of Tectonics
Earth Science Board
University of California, Santa Cruz
Santa Cruz, CA 95064

Prof. Arthur Lerner-Lam
Lamont-Doherty Geological Observatory
of Columbia University
Palisades, NY 10964

Dr. Christopher Lynnes
Teledyne Geotech
314 Montgomery Street
Alexandria, VA 22314

Prof. Peter Malin
University of California at Santa Barbara
Institute for Crustal Studies
Santa Barbara, CA 93106

Dr. Randolph Martin, III
New England Research, Inc.
76 Olcott Drive
White River Junction, VT 05001

Dr. Gary McCartor
Mission Research Corporation
735 State Street
P.O. Drawer 719
Santa Barbara, CA 93102 (2 copies)

Prof. Thomas V. McEvilly
Seismographic Station
University of California
Berkeley, CA 94720

Dr. Keith L. McLaughlin
S-CUBED
A Division of Maxwell Laboratory
P.O. Box 1620
La Jolla, CA 92038-1620

Prof. William Menke
Lamont-Doherty Geological Observatory
of Columbia University
Palisades, NY 10964

Stephen Miller
SRI International
333 Ravenswood Avenue
Box AF 116
Menlo Park, CA 94025-3493

Prof. Bernard Minster
IGPP, A-025
Scripps Institute of Oceanography
University of California, San Diego
La Jolla, CA 92093

Prof. Brian J. Mitchell
Department of Earth & Atmospheric Sciences
St. Louis University
St. Louis, MO 63156

Mr. Jack Murphy
S-CUBED, A Division of Maxwell Laboratory
11800 Sunrise Valley Drive
Suite 1212
Reston, VA 22091 (2 copies)

Dr. Bao Nguyen
GL/LWH
Hanscom AFB, MA 01731-5000

Prof. John A. Orcutt
IGPP, A-025
Scripps Institute of Oceanography
University of California, San Diego
La Jolla, CA 92093

Prof. Keith Priestley
University of Cambridge
Bullard Labs, Dept. of Earth Sciences
Madingley Rise, Madingley Rd.
Cambridge CB3 OEZ, ENGLAND

Prof. Paul G. Richards
L-210
Lawrence Livermore National Laboratory
Livermore, CA 94550

Dr. Wilmer Rivers
Teledyne Geotech
314 Montgomery Street
Alexandria, VA 22314

Prof. Charles G. Sammis
Center for Earth Sciences
University of Southern California
University Park
Los Angeles, CA 90089-0741

Prof. Christopher H. Scholz
Lamont-Doherty Geological Observatory
of Columbia University
Palisades, NY 10964

Prof. David G. Simpson
Lamont-Doherty Geological Observatory
of Columbia University
Palisades, NY 10964

Dr. Jeffrey Stevens
S-CUBED
A Division of Maxwell Laboratory
P.O. Box 1620
La Jolla, CA 92038-1620

Prof. Brian Stump
Institute for the Study of Earth & Man
Geophysical Laboratory
Southern Methodist University
Dallas, TX 75275

Prof. Jeremiah Sullivan
University of Illinois at Urbana-Champaign
Department of Physics
1110 West Green Street
Urbana, IL 61801

Prof. Clifford Thurber
University of Wisconsin-Madison
Department of Geology & Geophysics
1215 West Dayton Street
Madison, WS 53706

Prof. M. Nafi Toksoz
Earth Resources Lab
Massachusetts Institute of Technology
42 Carleton Street
Cambridge, MA 02142

Prof. John E. Vidale
University of California at Santa Cruz
Seismological Laboratory
Santa Cruz, CA 95064

Prof. Terry C. Wallace
Department of Geosciences
Building #77
University of Arizona
Tucson, AZ 85721

Dr. Raymond Willeman
GL/LWH
Hanscom AFB, MA 01731-5000

Dr. Lorraine Wolf
GL/LWH
Hanscom AFB, MA 01731-5000

Prof. Francis T. Wu
Department of Geological Sciences
State University of New York
at Binghamton
Vestal, NY 13901

OTHERS (United States)

Dr. Monem Abdel-Gawad
Rockwell International Science Center
1049 Camino Dos Rios
Thousand Oaks, CA 91360

Prof. Keiiti Aki
Center for Earth Sciences
University of Southern California
University Park
Los Angeles, CA 90089-0741

Prof. Shelton S. Alexander
Geosciences Department
403 Deike Building
The Pennsylvania State University
University Park, PA 16802

Dr. Kenneth Anderson
BBNSTC
Mail Stop 14/1B
Cambridge, MA 02238

Dr. Ralph Archuleta
Department of Geological Sciences
University of California at Santa Barbara
Santa Barbara, CA 93102

Dr. Thomas C. Bache, Jr.
Science Applications Int'l Corp.
10210 Campus Point Drive
San Diego, CA 92121 (2 copies)

J. Barker
Department of Geological Sciences
State University of New York
at Binghamton
Vestal, NY 13901

Dr. T.J. Bennett
S-CUBED
A Division of Maxwell Laboratory
11800 Sunrise Valley Drive, Suite 1212
Reston, VA 22091

Mr. William J. Best
907 Westwood Drive
Vienna, VA 22180

Dr. N. Biswas
Geophysical Institute
University of Alaska
Fairbanks, AK 99701

Dr. G.A. Bollinger
Department of Geological Sciences
Virginia Polytechnical Institute
21044 Derring Hall
Blacksburg, VA 24061

Dr. Steven R. Bratt
Center for Seismic Studies
1300 North 17th St., Suite 1450
Arlington, VA 22209

Michael Browne
Teledyne Geotech
3401 Shiloh Road
Garland, TX 75041

Mr. Roy Burger
1221 Serry Road
Schenectady, NY 12309

Dr. Robert Burridge
Schlumberger-Doll Research Center
Old Quarry Road
Ridgefield, CT 06877

Dr. Jerry Carter
Rondout Associates
P.O. Box 224
Stone Ridge, NY 12484

Dr. W. Winston Chan
Teledyne Geotech
314 Montgomery Street
Alexandria, VA 22314-1581

Dr. Theodore Cherry
Science Horizons, Inc.
710 Encinitas Blvd., Suite 200
Encinitas, CA 92024 (2 copies)

Prof. Jon F. Claerbout
Department of Geophysics
Stanford University
Stanford, CA 94305

Prof. Robert W. Clayton
Seismological Laboratory
Division of Geological & Planetary Sciences
California Institute of Technology
Pasadena, CA 91125

Prof. F. A. Dahlen
Geological and Geophysical Sciences
Princeton University
Princeton, NJ 08544-0636

Prof. Adam Dziewonski
Hoffman Laboratory
Harvard University
20 Oxford St
Cambridge, MA 02138

Prof. John Ebel
Department of Geology & Geophysics
Boston College
Chestnut Hill, MA 02167

Eric Fielding
SNEE Hall
INSTOC
Cornell University
Ithaca, NY 14853

Prof. Donald Forsyth
Department of Geological Sciences
Brown University
Providence, RI 02912

Dr. Cliff Frolich
Institute of Geophysics
8701 North Mopac
Austin, TX 78759

Prof. Art Frankel
Mail Stop 922
Geological Survey
790 National Center
Reston, VA 22092

Dr. Anthony Gangi
Texas A&M University
Department of Geophysics
College Station, TX 77843

Dr. Freeman Gilbert
Inst. of Geophysics & Planetary Physics
University of California, San Diego
P.O. Box 109
La Jolla, CA 92037

Mr. Edward Giller
Pacific Sierra Research Corp.
1401 Wilson Boulevard
Arlington, VA 22209

Dr. Jeffrey W. Given
Sierra Geophysics
11255 Kirkland Way
Kirkland, WA 98033

Prof. Stephen Grand
University of Texas at Austin
Department of Geological Sciences
Austin, TX 78713-7909

Prof. Roy Greenfield
Geosciences Department
403 Deike Building
The Pennsylvania State University
University Park, PA 16802

Dan N. Hagedorn
Battelle
Pacific Northwest Laboratories
Battelle Boulevard
Richland, WA 99352

Kevin Hutchenson
Department of Earth Sciences
St. Louis University
3507 Laclede
St. Louis, MO 63103

Prof. Thomas H. Jordan
Department of Earth, Atmospheric
and Planetary Sciences
Massachusetts Institute of Technology
Cambridge, MA 02139

Robert C. Kemerait
ENSCO, Inc.
445 Pineda Court
Melbourne, FL 32940

William Kikendall
Teledyne Geotech
3401 Shiloh Road
Garland, TX 75041

Prof. Leon Knopoff
University of California
Institute of Geophysics & Planetary Physics
Los Angeles, CA 90024

Prof. L. Timothy Long
School of Geophysical Sciences
Georgia Institute of Technology
Atlanta, GA 30332

Prof. Art McGarr
Mail Stop 977
Geological Survey
345 Middlefield Rd.
Menlo Park, CA 94025

Dr. George Mellman
Sierra Geophysics
11255 Kirkland Way
Kirkland, WA 98033

Prof. John Nabelek
College of Oceanography
Oregon State University
Corvallis, OR 97331

Prof. Geza Nagy
University of California, San Diego
Department of Ames, M.S. B-010
La Jolla, CA 92093

Prof. Amos Nur
Department of Geophysics
Stanford University
Stanford, CA 94305

Prof. Jack Oliver
Department of Geology
Cornell University
Ithaca, NY 14850

Prof. Robert Phinney
Geological & Geophysical Sciences
Princeton University
Princeton, NJ 08544-0636

Dr. Paul Pomeroy
Rondout Associates
P.O. Box 224
Stone Ridge, NY 12484

Dr. Jay Pulli
RADIX System, Inc.
2 Taft Court, Suite 203
Rockville, MD 20850

Dr. Norton Rimer
S-CUBED
A Division of Maxwell Laboratory
P.O. Box 1620
La Jolla, CA 92038-1620

Prof. Larry J. Ruff
Department of Geological Sciences
1006 C.C. Little Building
University of Michigan
Ann Arbor, MI 48109-1063

Dr. Richard Sailor
TASC Inc.
55 Walkers Brook Drive
Reading, MA 01867

Thomas J. Sereno, Jr.
Science Application Int'l Corp.
10210 Campus Point Drive
San Diego, CA 92121

John Sherwin
Teledyne Geotech
3401 Shiloh Road
Garland, TX 75041

Prof. Robert Smith
Department of Geophysics
University of Utah
1400 East 2nd South
Salt Lake City, UT 84112

Prof. S. W. Smith
Geophysics Program
University of Washington
Seattle, WA 98195

Dr. Stewart Smith
IRIS Inc.
1616 North Fort Myer Drive
Suite 1440
Arlington, VA 22209

Dr. George Sutton
Rondout Associates
P.O. Box 224
Stone Ridge, NY 12484

Prof. L. Sykes
Lamont-Doherty Geological Observatory
of Columbia University
Palisades, NY 10964

Prof. Pradeep Talwani
Department of Geological Sciences
University of South Carolina
Columbia, SC 29208

Prof. Ta-liang Teng
Center for Earth Sciences
University of Southern California
University Park
Los Angeles, CA 90089-0741

Dr. R.B. Tittmann
Rockwell International Science Center
1049 Camino Dos Rios
P.O. Box 1085
Thousand Oaks, CA 91360

Dr. Gregory van der Vink
IRIS, Inc.
1616 North Fort Myer Drive
Suite 1440
Arlington, VA 22209

Professor Daniel Walker
University of Hawaii
Institute of Geophysics
Honolulu, HI 96822

William R. Walter
Seismological Laboratory
University of Nevada
Reno, NV 89557

Dr. Gregory Wojcik
Weidlinger Associates
4410 El Camino Real
Suite 110
Los Altos, CA 94022

Prof. John H. Woodhouse
Hoffman Laboratory
Harvard University
20 Oxford St.
Cambridge, MA 02138

Dr. Gregory B. Young
ENSCO, Inc.
5400 Port Royal Road
Springfield, VA 22151-2388

Dr. Ralph Alewine III
DARPA/NMRO
1400 Wilson Boulevard
Arlington, VA 22209-2308

Mr. James C. Battis
GL/LWH
Hanscom AFB, MA 01731-5000

Dr. Robert Blandford
DARPA/NMRO
1400 Wilson Boulevard
Arlington, VA 22209-2308

Eric Chael
Division 9241
Sandia Laboratory
Albuquerque, NM 87185

Dr. John J. Cipar
GL/LWH
Hanscom AFB, MA 01731-5000

Mr. Jeff Duncan
Office of Congressman Markey
2133 Rayburn House Bldg.
Washington, DC 20515

Dr. Jack Evernden
USGS - Earthquake Studies
345 Middlefield Road
Menlo Park, CA 94025

Art Frankel
USGS
922 National Center
Reston, VA 22092

Dr. T. Hanks
USGS
Nat'l Earthquake Research Center
345 Middlefield Road
Menlo Park, CA 94025

Dr. James Hannon
Lawrence Livermore Nat'l Laboratory
P.O. Box 808
Livermore, CA 94550

Paul Johnson
ESS-4, Mail Stop J979
Los Alamos National Laboratory
Los Alamos, NM 87545

Janet Johnston
GL/LWH
Hanscom AFB, MA 01731-5000

Dr. Katharine Kadinsky-Cade
GL/LWH
Hanscom AFB, MA 01731-5000

Ms. Ann Kerr
IGPP, A-025
Scripps Institute of Oceanography
University of California, San Diego
La Jolla, CA 92093

Dr. Max Koontz
US Dept of Energy/DP 5
Forrestal Building
1000 Independence Avenue
Washington, DC 20585

Dr. W.H.K. Lee
Office of Earthquakes, Volcanoes,
& Engineering
345 Middlefield Road
Menlo Park, CA 94025

Dr. William Leith
U.S. Geological Survey
Mail Stop 928
Reston, VA 22092

Dr. Richard Lewis
Director, Earthquake Engineering & Geophysics
U.S. Army Corps of Engineers
Box 631
Vicksburg, MS 39180

James F. Lewkowicz
GL/LWH
Hanscom AFB, MA 01731-5000

Mr. Alfred Lieberman
ACDA/VI-OA'State Department Bldg
Room 5726
320 - 21st Street, NW
Washington, DC 20451

Stephen Mangino
GL/LWH
Hanscom AFB, MA 01731-5000

Dr. Robert Masse
Box 25046, Mail Stop 967
Denver Federal Center
Denver, CO 80225

Art McGarr
U.S. Geological Survey, MS-977
345 Middlefield Road
Menlo Park, CA 94025

Richard Morrow
ACDA/VI, Room 5741
320 21st Street N.W
Washington, DC 20451

Dr. Keith K. Nakanishi
Lawrence Livermore National Laboratory
P.O. Box 808, L-205
Livermore, CA 94550

Dr. Carl Newton
Los Alamos National Laboratory
P.O. Box 1663
Mail Stop C335, Group ESS-3
Los Alamos, NM 87545

Dr. Kenneth H. Olsen
Los Alamos Scientific Laboratory
P.O. Box 1663
Mail Stop C335, Group ESS-3
Los Alamos, NM 87545

Howard J. Patton
Lawrence Livermore National Laboratory
P.O. Box 808, L-205
Livermore, CA 94550

Mr. Chris Paine
Office of Senator Kennedy
SR 315
United States Senate
Washington, DC 20510

Colonel Jerry J. Perrizo
AFOSR/NP, Building 410
Bolling AFB
Washington, DC 20332-6448

Dr. Frank F. Pilotte
HQ AFTAC/TT
Patrick AFB, FL 32925-6001

Katie Poley
CIA-OSWR/NED
Washington, DC 20505

Mr. Jack Rachlin
U.S. Geological Survey
Geology, Rm 3 C136
Mail Stop 928 National Center
Reston, VA 22092

Dr. Robert Reinke
WL/NTESG
Kirtland AFB, NM 87117-6008

Dr. Byron Ristvet
HQ DNA, Nevada Operations Office
Attn: NVCG
P.O. Box 98539
Las Vegas, NV 89193

Dr. George Rothe
HQ AFTAC/TGR
Patrick AFB, FL 32925-6001

Dr. Alan S. Ryall, Jr.
DARPA/NMRO
1400 Wilson Boulevard
Arlington, VA 22209-2308

Dr. Michael Shore
Defense Nuclear Agency/SPSS
6801 Telegraph Road
Alexandria, VA 22310

Donald L. Springer
Lawrence Livermore National Laboratory
P.O. Box 808, L-205
Livermore , CA 94550

Mr. Charles L. Taylor
GL/LWG
Hanscom AFB, MA 01731-5000

Dr. Thomas Weaver
Los Alamos National Laboratory
P.O. Box 1663, Mail Stop C335
Los Alamos, NM 87545

J.J. Zucca
Lawrence Livermore National Laboratory
Box 808
Livermore, CA 94550

GL/SULL
Research Library
Hanscom AFB , MA 01731-5000 (2 copies)

Secretary of the Air Force
(SAFRD)

Washington, DC 20330

Office of the Secretary Defense
DDR & E
Washington, DC 20330

HQ DNA
Attn: Technical Library
Washington, DC 20305

DARPA/RMO/RETRIEVAL
1400 Wilson Boulevard
Arlington, VA 22209

DARPA/RMO/Security Office
1400 Wilson Boulevard
Arlington, VA 22209

Geophysics Laboratory
Attn: XO
Hanscom AFB, MA 01731-5000

Geophysics Laboratory
Attn: LW
Hanscom AFB, MA 01731-5000

DARPA/PM
1400 Wilson Boulevard
Arlington, VA 22209

Defense Technical Information Center
Cameron Station
Alexandria, VA 22314 (5 copies)

Defense Intelligence Agency
Directorate for Scientific &
Technical Intelligence/DT1B
Washington, DC 20340-6158

AFTAC/CA
(STINFO)
Patrick AFB, FL 32925-6001

TACTEC
Battelle Memorial Institute
505 King Avenue
Columbus, OH 43201 (Final Report Only)

CONTRACTORS (Foreign)

Dr. Ramon Cabre, S.J.
Observatorio San Calixto
Casilla 5939
La Paz, Bolivia

Prof. Hans-Peter Harjes
Institute for Geophysik
Ruhr University/Bochum
P.O. Box 102148
4630 Bochum 1, FRG

Prof. Eystein Husebye
NTNF/NORSAR
P.O. Box 51
N-2007 Kjeller, NORWAY

Prof. Brian L.N. Kennett
Research School of Earth Sciences
Institute of Advanced Studies
G.P.O. Box 4
Canberra 2601, AUSTRALIA

Dr. Bernard Massinon
Societe Radiomana
27 rue Claude Bernard
75005 Paris, FRANCE (2 Copies)

Dr. Pierre Mecheler
Societe Radiomana
27 rue Claude Bernard
75005 Paris, FRANCE

Dr. Svein Mykkeltveit
NTNF/NORSAR
P.O. Box 51
N-2007 Kjeller, NORWAY

FOREIGN (Others)

Dr. Peter Basham
Earth Physics Branch
Geological Survey of Canada
1 Observatory Crescent
Ottawa, Ontario, CANADA K1A 0Y3

Dr. Eduard Berg
Institute of Geophysics
University of Hawaii
Honolulu, HI 96822

Dr. Michel Bouchon
I.R.I.G.M.-B.P. 68
38402 St. Martin D'Heres
Cedex, FRANCE

Dr. Hilmar Bungum
NTNF/NORSAR
P.O. Box 51
N-2007 Kjeller, NORWAY

Dr. Michel Campillo
Observatoire de Grenoble
I.R.I.G.M.-B.P. 53
38041 Grenoble, FRANCE

Dr. Kin Yip Chun
Geophysics Division
Physics Department
University of Toronto
Ontario, CANADA M5S 1A7

Dr. Alan Douglas
Ministry of Defense
Blacknest, Brimpton
Reading RG7-4RS, UNITED KINGDOM

Dr. Roger Hansen
NTNF/NORSAR
P.O. Box 51
N-2007 Kjeller, NORWAY

Dr. Manfred Henger
Federal Institute for Geosciences & Nat'l Res.
Postfach 510153
D-3000 Hanover 51, FRG

Ms. Eva Johannisson
Senior Research Officer
National Defense Research Inst.
P.O. Box 27322
S-102 54 Stockholm, SWEDEN

Dr. Fekadu Kebede
Seismological Section
Box 12019
S-750 Uppsala, SWEDEN

Dr. Tormod Kvaerna
NTNF/NORSAR
P.O. Box 51
N-2007 Kjeller, NORWAY

Dr. Peter Marshal
Procurement Executive
Ministry of Defense
Blacknest, Brimpton
Reading FG7-4RS, UNITED KINGDOM

Prof. Ari Ben-Menahem
Department of Applied Mathematics
Weizman Institute of Science
Rehovot, ISRAEL 951729

Dr. Robert North
Geophysics Division
Geological Survey of Canada
1 Observatory Crescent
Ottawa, Ontario, CANADA K1A 0Y3

Dr. Frode Ringdal
NTNF/NORSAR
P.O. Box 51
N-2007 Kjeller, NORWAY

Dr. Jorg Schlittenhardt
Federal Institute for Geosciences & Nat'l Res.
Postfach 510153
D-3000 Hannover 51, FEDERAL REPUBLIC OF GERMANY